Stochastic Modeling and Optimization to Improve Identification and Treatment of Alzheimer's Disease

by

Raquel Camarena
for the Alzheimer's Disease Neuroimaging Initiative*

A Thesis Presented in Partial Fulfillment
of the Requirements for the Degree
Master of Science

Approved May 2018 by the
Graduate Supervisory Committee:

Giulia Pedrielli, Co-Chair
Jing Li, Co-Chair
Teresa Wu

ARIZONA STATE UNIVERSITY

August 2018

*Data used in preparation of this Thesis were obtained from the Alzheimer's Disease Neuroimaging Initiative (ADNI) database (adni.loni.usc.edu). As such, the investigators within the ADNI contributed to the design and implementation of ADNI and/or provided data but did not participate in analysis or writing of this report. A complete listing of ADNI investigators can be found at: http://adni.loni.usc.edu/wp-content/uploads/how_to_apply/ADNI_Acknowledgement_List.pdf.

ABSTRACT

Mathematical modeling and decision-making within the healthcare industry have given means to quantitatively evaluate the impact of decisions into diagnosis, screening, and treatment of diseases. In this work, we look into a specific, yet very important disease, the Alzheimer. In the United States, Alzheimer's Disease (AD) is the 6^{th} leading cause of death. Diagnosis of AD cannot be confidently confirmed until after death. This has prompted the importance of early diagnosis of AD, based upon symptoms of cognitive decline. A symptom of early cognitive decline and indicator of AD is Mild Cognitive Impairment (MCI). In addition to this qualitative test, Biomarker tests have been proposed in the medical field including p-Tau, FDG-PET, and hippocampal. These tests can be administered to patients as early detectors of AD thus improving patients' life quality and potentially reducing the costs of the health structure. Preliminary work has been conducted in the development of a Sequential Tree Based Classifier (STC), which helps medical providers predict if a patient will contract AD or not, by sequentially testing these biomarker tests. The STC model, however, has its limitations and the need for a more complex, robust model is needed. In fact, STC assumes a general linear model as the status of the patient based upon the tests results. We take a simulation perspective and try to define a more complex model that represents the patient evolution in time.

Specifically, this thesis focuses on the formulation of a Markov Chain model that is complex and robust. This Markov Chain model emulates the evolution of MCI patients based upon doctor visits and the sequential administration of biomarker tests. Data provided to create this Markov Chain model were collected by the Alzheimer's Disease

Neuroimaging Initiative[1] (ADNI) database. The data lacked detailed information of the sequential administration of the biomarker tests and therefore, different analytical approaches were tried and conducted in order to calibrate the model. The resulting Markov Chain model provided the capability to conduct experiments regarding different parameters of the Markov Chain and yielded different results of patients that contracted AD and those that did not, leading to important insights into effect of thresholds and sequence on patient prediction capability as well as health costs reduction.

[1] The data in this thesis was provided from the Alzheimer's Disease Neuroimaging Initiative (ADNI) database (adni.loni.usc.edu). ADNI investigators did not contribute to any analysis or writing of this thesis. A list of the ADNI investigators can be found at: http://adni.loni.usc.edu/about/governance/principal-investigators/ .

ACKNOWLEDGEMENTS

I would like to thank my Committee Chair, Dr. Giulia Pedrielli. Her patience and help throughout this research was much appreciated. It has been a privilege to learn and work with her. I also want to thank my Co-Chair, Dr. Jing Li, for allowing me to consult on this project that she owns. Additionally, I want to thank and acknowledge the help I have received from students, Bing Si and Logan Mathesen. Both helped me throughout this research by answering questions about data interpretation, code explanation, and aided in developing necessary code. I further want to thank my committee member Dr. Teresa Wu for her time and assistance. I lastly, would like to thank my family for their support and encouragement.

This Thesis was able to be conducted due to the funding by the Alzheimer's Disease Neuroimaging Initiative (ADNI) (National Institutes of Health Grant U01 AG024904) and DOD ADNI (Department of Defense award number W81XWH-12-2-0012). This funding has provided the data collection and ability to share data. ADNI is funded by the National Institute on Aging, the National Institute of Biomedical Imaging and Bioengineering, and through generous contributions from the following: AbbVie, Alzheimer's Association; Alzheimer's Drug Discovery Foundation; Araclon Biotech; BioClinica, Inc.; Biogen; Bristol-Myers Squibb Company; CereSpir, Inc.; Cogstate; Eisai Inc.; Elan Pharmaceuticals, Inc.; Eli Lilly and Company; EuroImmun; F. Hoffmann-La Roche Ltd and its affiliated company Genentech, Inc.; Fujirebio; GE Healthcare; IXICO Ltd.; Janssen Alzheimer Immunotherapy Research & Development, LLC.; Johnson & Johnson

Pharmaceutical Research & Development LLC.; Lumosity; Lundbeck; Merck & Co., Inc.; Meso Scale Diagnostics, LLC.; NeuroRx Research; Neurotrack Technologies; Novartis Pharmaceuticals Corporation; Pfizer Inc.; Piramal Imaging; Servier; Takeda Pharmaceutical Company; and Transition Therapeutics. In Canada, ADNI's funds are provided by the Canadian Institute of Health Research. The Foundation for the National Institutes of Health (www.fnih.org) facilitates private sector contributions. Northern California Institute for Research and Education is the grantee organization and the study is organized by the Alzheimer's Therapeutic Research Institute at the University of Southern California. ADNI data are distributed by the Laboratory for Neuro Imaging at the University of Southern California.

TABLE OF CONTENTS

CHAPTER Page

LIST OF TABLES

LIST OF FIGURES

CHAPTER 1: INTRODUCTION

1.1 Alzheimer's Disease Background

Alzheimer's Disease (AD) is a neurodegenerative disease that impacts an individual's memory, language, and reasoning. AD, as of 2012, has affected more than 35 million individuals across the world and within the United States has affected over 5 million individuals [1]. The spread of the disease has led to prioritize research of preventing AD [2]. AD cannot be definitively diagnosed until after death and thus can only be likely diagnosed [2]. Therefore, individuals are first diagnosed with symptoms of dementia or most noticeably diagnosed as Mild Cognitive Impairment (MCI). Dementia and MCI are the first indicators of cognitive decline [2,3].

The National Institute on Aging-Alzheimer's Association (NIA-AA) has conducted and recommended research into criteria for MCI to AD conversion that incorporate the use of the following biomarkers: P-tau- phosphorylate tau level measured by cerebrospinal fluid (CSF), FDG- measured by an FDG-PET scan, and Hippo- hippocampal volume measured by an MRI [3, 4]. In the *Journal of Alzheimer's Disease* an international panel of experts came together to declare that the identification and detection of AD risk factors are important in AD prevention [5]. Utilizing these biomarkers to accurately predict the conversion of MCI to AD can help with the early detection of AD.

There have been studies using biomarkers to predict the conversion from MCI to AD [3]. However, these past studies have had limitations as their prediction accuracy has been unsuitable and the costs associated to these biomarkers as well as the time required for diagnosis results in a long period of time with effects on patients' quality of life and

financial inefficiencies for the medical structures. One of the issues causing the aforementioned inefficiencies resides in the common approach to propose a single model for all patients. In fact, the single model assumption may result into challenges due to the inherent differences between patients due to, for example, physical and genetic characteristics. Additionally, another limitation during these studies, is that most use classification techniques, and, as such, require all the test results to be known in order to apply any technique. In other words, these techniques are not able to embed the decision of which biomarker to test at which time. A classification model groups a set of interested subjects, such as patients into different classes based upon certain attributes [18]. Therefore, a classification model will map an input attribute (a new individual/patient), into its class label (output) [6]. In these studies, the creation of a classification model allowed researchers to group individuals into a class of converters and non-converters with inaccuracies discussed in [3]. Furthermore, having all biomarkers measured at once, is difficult to do because at medical institutions there are constraints that include: the necessary resources such as personnel and tests, not enough time to conduct these tests, and the high associated costs administering these biomarker tests. Lastly, another limitation was that these biomarkers predicted conversions of MCI to AD on a numerical scale, meaning there is a hard cutoff for measurements to establish if a patient is in the "positive" or "negative" side of the biomarker measurement. This also allows classification decisions to be susceptible to measurement errors and unwanted bias [4]. A new model has been developed to combat these limitations.

1.2 Preliminary Work (STC)

Si et al. in [3] proposed for the first time the Sequential Tree-Based Classifier (STC). The STC was designed to improve the prediction of conversion of MCI to AD and classify patients with their likelihood of conversions: High-Risk (HR), Low-Risk (LR), and inconclusive. To categorize these conversions, two biomarker cutoffs were proposed allowing to separate High-Risk (HR) and Low-Risk (LR) patients. In order to perform such prediction, the STC approach considers the biomarker values, the sequence at which the tests were taken, additional covariates that characterize patients such as age, sex and MCI outcome. Applied to each patient, the STC produces a personalized judgment of how the patient should be categorized by producing a personalized pair of thresholds [4]. Specifically, these thresholds are generated assuming that the biomarker value X is a linear function of the covariates and the true (unknown) class of the patient (i.e., converter/non-converter). The model used in [3] is:

$$X_i = \beta_{0,i} + \beta_{y,i} Y + \beta_{z,i}^T Z + \varepsilon \sim N(0, \sigma^2) \quad (1)$$

Where X_i is the type of biomarker test, Z identifies the risk factors within a sub cohort of patients (i.e. gender, age, etc.), Y determines the type of patient outcome, if $Y = 1$, the patient converts from MCI to AD and if $Y = 0$ then the patient does not. Within this outcome, the biomarkers cutoffs for HR and LR will further classify patients based upon how likely they will convert from MCI to AD. The formulation allows to compare several test sequences, thus determining, in turn the optimal sequence that maximizes the accuracy

in the classification of the patient while controlling the overall testing costs. Once the cutoffs are established the patients will be classified as either HR if they exceed the upper cutoff, LR if they are below the lower cutoff, and inconclusive if they do not fall above or below a certain cutoff. Biomarkers will no longer need to be tested once the patients have been classified as HR or LR, but if the patients are classified as inconclusive, then they must be tested for the next biomarker in the sequence. This sequence will continue until all biomarkers are tested for the inconclusive patients.

1.3 STC Challenges

Due to this preliminary work there exists challenges. This type of model is generalized and takes the assumption that there is a linear relationship between the response variable X_i and its factors Y and Z. The STC does not consider the dependency and interaction among the biomarker tests. This can impact the response variable, X_i. The response can result as nonlinear, inconsistent standard deviation due to different values of the covariates (Y and Z), skewed responses, and non-normally distributed errors [7]. Due to the current setup of the STC model, the sequence is fixed, meaning all patients must go through the same sequence. In the following literature reviews, the purpose for modeling healthcare diseases such as AD will be highlighted.

CHAPTER 2: LITERATURE REVIEW

2.1 Introduction

The healthcare industry has vast opportunities for applying decision making models such as STC. The following literature review was written to determine the current applications for Medical Decision Making (MDM) as well as determine how a specific

type of modeling known as Markov Chains (MC) can be utilized in healthcare. The first section discusses how Operations Research methodologies can be applied to decision making. The second section walks through the Markov Chain modeling of HIV/AIDS progression. Similar to the second section, this research will use a Markov Chain to model the progression of AD.

2.2 Decision Making in Healthcare

Healthcare costs in the United States continue to rise. In 2014, the US health cost exceeded $2.5 trillion [8]. It is projected that these costs will exceed other gross domestic price (GDP) categories [8]. Along with the issue of the rise of costs, the impact to individuals is just as severe as diseases continue to impact all persons of all backgrounds. Everyday medical decisions must be made by doctors that impact the diagnosis and treatment of patients. These decisions rely on quantitative models and some applications from quantitative models include: breast cancer diagnosis and treatment, disease modeling, drug selection for HIV treatment, optimization of the timing of organ transplants, and the optimization of radiotherapy treatment [8].

Modeling of Medical Decision Making (MDM) has become popular because past statistics demonstrate that medical errors due to poor decision making has attributed to a leading cause of death. A 1999 report stated that medical errors were responsible for approximately 100,000 deaths each year. From these deaths medical costs equated about in about $37.6 billion and of that, approximately $17 billion were because of preventable errors [8]. Additionally, MDM has become popular due to the increase in technology that allows medical doctors and personnel to collect medical information about the patient. This

technology gives researchers opportunities to model diseases, treatments, and optimizations more efficiently due to the vast amount of data available.

Currently healthcare policy decision makers use ad-hoc and heuristic decision-making methodologies. These approaches currently are not capable of incorporating the complexity that comes along with the diagnosis, screening, and treatment of patients that have uncertain factors [8]. Therefore, it is important that Operations Research (OR) methodologies be used to combat these complex factors. OR is defined as utilizing complex analytical methods to make decisions. OR can be useful in healthcare and making decisions because complex healthcare problems can be modeled by considering the rationalization and the uncertain effects of making a certain decision based upon a patient's needs [8].

The interest of MDM in OR is due to the need of sequential decision making under unpredictable factors [8]. Sequential decision making occurs because there are various options and decisions that doctors must make in terms of their patient's health state [8]. Doctor's decisions rely on past situations and decisions [8]. Some examples of unpredictability include a patient's response to: chemotherapy, antibiotics, and access to limited resources such as transplant organs [8].

Case studies have been applied the usage of MDM. In one case study MDM examined the process of the screening of a mammography [8]. The decision that needed to be determined was when a mammogram needed to be sent for biopsy [8]. This decision was based upon the factors of the mammogram and the patient's demographics [8]. In this case study researchers determined optimal biopsy thresholds that helped determine the optimal time to send the mammograms for a biopsy [8]. A second case study of MDM

studied the ability to develop a personalized mammography screening schedule. This schedule used past screening history and the patient's personal risk characteristics [8]. This case study highlights the application of individualized patient care MDM can bring. The final case study mentioned is on making optimal decisions from resource constraints. Pertaining to mammograms an approach that was developed optimized thresholds over traditional methods and ultimately saved costs [8].

Applying OR methods to MDM is still developing [8]. Major research problems that MDM is tackling include: personalized patient care due to prognosis and treatment, quantitative behavior modeling of patients, and optimizing communications between medical professionals and patients [8]. In this paper, the process of making decisions pertaining to ordering prognosis biomarker tests is studied. It is crucial to understand and optimize the administration of these biomarker tests because the earliest of detection of AD the better for effective treatment and it will reduce the costs of unnecessary tests.

2.3 Markov Chain Modeling in Healthcare

In the related literature, a Markov Chain was used to forecast the progression of HIV/AIDS of African Americans and Caucasian Americans [9]. This type of modeling was used to project the number of African Americans and Caucasian Americans that are diagnosed with AIDS and HIV and predicts those that will be dead in the year 2030 [9].

Markov Chain models are used because of the ability to embed stochastic factors. A Markov Chain follows the characteristics of a Markov process. A Markov process is a stochastic process. A stochastic process occurs when a system changes unpredictably between different states [9]. Markov processes are frequently used to tackle healthcare

topics such as: genetics, determining the potency of diabetes, predicting kidney transplants, and analyzing disease progressions for liver cancer, breast cancer, and Alzheimer's Disease [9]. These healthcare topics possess stochastic factors and are suitable to be modeled by a Markov Chain because of its ability to model stochastic factors.

As an example, HIV/AIDS progression has been modeled as a discrete time Markov Chain with stationary transition probabilities [9]. Due to this assumption, the Markovian property is satisfied. The Markovian Property states that the probability of a random variable being in a state during a period in time only depends on the prior state before it and not on any other state [9]. Because of this property a Markov Chain model is useful to model unpredictable progression behavior even without a lot of past historical data [9]. Lee, Ko, Patel, Balkrishnan, and Chang et al. in [9] predicted, using the Markov Chain model, that Caucasian Americans currently living with HIV/AIDS is smaller than African Americans, but predictions show that the number of Caucasian Americans with HIV/AIDS will continue to increase [9].

The methodology of formulating a Markov Chain conducted in this literature and explained in this section, follows the same procedure that will be explained in Chapter 3. The formulation of a Markov Chain needs states, transition probabilities, and the modeled data statistics for verification of the Markov Chain model's results. Formulating a Markov Chain begins by establishing states. The states modeled in this literature follow the state notation: $S = S_1, S_2, \dots, S_n$. S_1 = the rate of vulnerable people (V), S_2 = the rate of people diagnosed with HIV (H), S_3 = the rate of people diagnosed with AIDS (A), S_4 = the rate of deaths from HIV/AIDS (D). States S_1, S_2, and S_3 are modeled as transient states and S_4 is

modeled as an absorbing state [9]. Transient states are states that the patient can transition into and out of and an absorbing state is when the patient will never transition out of that state. The following figure represents the transitions among the different states.

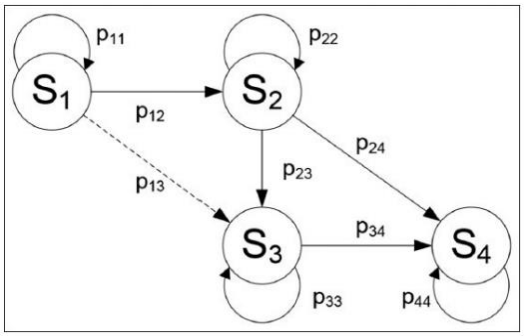

Figure 1: Transition Diagram for HIV/AIDS (Source [9])

The next step in modeling a Markov Chain would be to use the provided data for the model formulation. In this literature study, four years of data (2006-2009) from the Centers of Disease Control and Prevention (CDC) and the Prevention HIV/AIDS Surveillance Report from 2009 were used. This data provided the rates of African Americans and Caucasian Americas for each state. These rates then were calculated to their respective transition probabilities. These transition probabilities are represented in Figure 1 with the notation of p_{ij}, where i represents the prior state and j represents the next state. Two different transition matrices were constructed, T_B = African Americans and T_W= Caucasian Americans.

$$T_B = \begin{bmatrix} 0.99893 & 0.00066 & 0.00041 & 0 \\ 0 & 0.97033 & 0.00005 & 0.02962 \\ 0 & 0 & 0.95776 & 0.04224 \\ 0 & 0 & 0 & 1 \end{bmatrix}$$

Figure 2: African American Transition Matrix (Source [9])

$$T_W = \begin{bmatrix} 0.9998787 & 0.0000733 & 0.0000480 & 0 \\ 0 & 0.9772259 & 0.0000015 & 0.0227725 \\ 0 & 0 & 0.9693415 & 0.0306585 \\ 0 & 0 & 0 & 1 \end{bmatrix}$$

Figure 3: Caucasian American Transition Matrix (Source [9])

The last step in modeling a Markov Chain would be to verify this model with the actual statistics of those affected with HIV/AIDS [9]. This verification allows the model to

be assessed on its accuracy in predicting and forecasting. This literature provided an overview of the needed elements in developing a Markov Chain model and informed the methodology process used in this thesis.

CHAPTER 3: METHODOLOGY

3.1 Method Overview

Due to the research goal of creating a Markov Chain model, the following work was outlined. The highlighted sections represent the focus of research conducted.

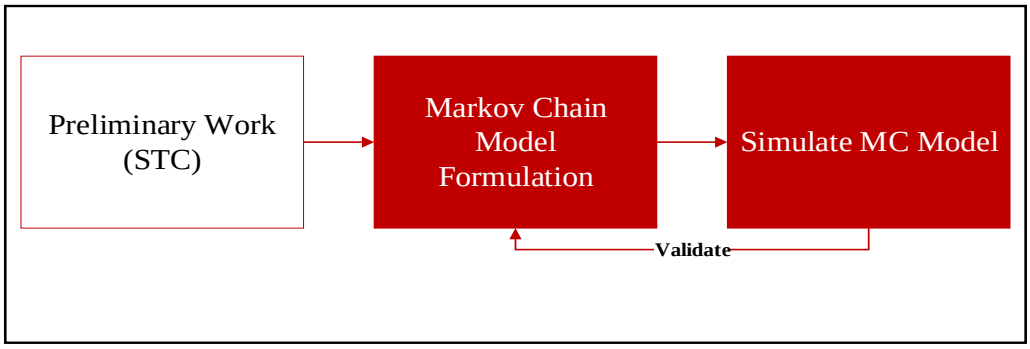

Figure 4: Method Overview

The basis of this research is the formulation of a Markov Chain model that models the evolution of MCI patients based upon doctor visits. This is done to create the benchmark needed to understand the impact of the sequential order of the administration of the biomarker tests decided by doctors. As mentioned in section 1.2 the STC model has its limitations of not being able to effectively model the dependency between the tests and the uncertainty characterizing the process if not through additive gaussian noise. The remaining part of this chapter will discuss the initial data used to create the Markov Chain model and will discuss the steps of formulating the Markov Chain model. Techniques and results will additionally be explained. Chapter 4 will discuss the simulation of the Markov

Chain model and the results of different experiments conducted. In conclusion, Chapter 5 will recap the purpose and objective of this research as well as its numerical results.

3.2 Data Description

The data used to create the Markov Chain model was obtained from the Alzheimer's Disease Neuroimaging Initiative (ADNI) database (adni.loni.usc.edu) on July 31st, 2013 [3]. The ADNI originated in 2003 as a public-private partnership, spearheaded from Michael W. Weiner, the Principal Investigator. The principal goal of ADNI has composed of testing whether serial magnetic resonance imaging (MRI), positron emission tomography (PET), other biological markers, and clinical and neuropsychological assessment can be accumulated to measure the progression of MCI and early AD. To obtain more information visit www.adni-info.org.

This Markov Chain model was created from a total of 144 patient's records. These 144 records reflected patients at the MCI stage and observed the patient's progression for two years of either contracting AD or not contracting AD. If a patient contracted AD, the value assigned to that specific patient and record was recorded as 1 and 0 otherwise. From these 144 records, 72 patients contracted AD and the other 72 patients did not convert to AD. All 144 records included the biomarker test ranges of p-Tau, FDG-PET, and Hippo. An example of the framework of this ADNI data is represented below.

Patient Number	Conversion-2 years	p-Tau	FDG-PET	Hippo
1	1	-	-	-
2	0	-	-	-
.	.	.	.	.
.	.	.	.	.
.	.	.	.	.

Table 1: ADNI Data Framework

3.3 Markov Chain Formulation

3.3.1 Assumptions

Due to the multiple factors of modeling the evolution of a patient's visits to the doctor, assumptions were made to create the Markov Chain model. The first assumption was that all patients belonged to same type of population and therefore all were considered homogeneous. The second assumption was that the doctors administered a specific biomarker test randomly. For example, if a patient was not given any tests yet, the patient had a $1/3$ chance of being administered the p-Tau test. Then if the patient still was not diagnosed of either contracting AD or not, another biomarker test would be randomly administered, and the remaining tests would be the FDG-PET and the Hippo test. If the next biomarker test administered was the FDG-PET test, the probability of that test being chosen would be $1/2$. Then the remaining probability of being administered the Hippo test would be 1.

3.3.2 States

States within a Markov Chain are dependent on the decision maker. The states of the system will be represented as an overall vector of X composed of vectors: X_T and X_H based upon the t^{th} doctor visit. The two vectors will represent the biomarker tests (X_T) and the patient's health state (X_H). The biomarker tests will consist of three tests: {p-Tau test, FDG-PET test, and a hippocampal (Hippo) test}. If a test in X_T was performed then it would take a value of 1, otherwise 0. The patient's health state after being administered a biomarker test will result in: contraction of AD, no contraction of AD, or inconclusive. The patient health states in X_H will take a value of the associated states in abbreviation form of:

no detection of AD = NAD, detection of AD = AD, and Inconclusive = I. Both vectors will be represented as an overall vector: $X = [X_H, X_T]$. The vectors are represented below.

Patient Health State Vector:

$X_H \epsilon \mathbb{R}^3$ =[no AD = NAD, AD = AD, Inconclusive = I]

Biomarker Test Vector:

$X_T \epsilon \mathbb{R}^3$ = [p-Tau, FDG-PET, Hippo]

$$X_T = \begin{cases} 1, & if\ corresponding\ test\ taken \\ 0, & otherwise \end{cases}$$

Overall Vector

$$X = [X_H, X_T] \tag{2}$$

Thus, the overall vector of both the biomarker test and the patient's health state will be mathematically represented as:

$$P(X_{t+1} = j \mid X_t = i) = p_{ij} \tag{3}$$

$t = 1,2, \ldots$ is the index of the visit.

Where i, j represents states at time t and p_{ij} represents the probability of the states after a transition from one state to another. For example, state, [1, 0, 1, AD] means that the p-Tau and the Hippo test were administered and the MCI patient contracted AD. By using a Markov Chain model, the future state of the patient can be predicted based upon the current state of the patient. This Markov Chain is based off the Stationary Assumption, where the transition states are independent of the doctor visit, t [10].

3.3.3 Transition Matrix and Diagram

Based upon the formulated states a transition matrix could be created. A total of 22 states existed. Each possible transition from each state was traced and formulated a 22 by 22 matrix. Within these transition states exists absorbing states. Absorbing states are states when the patient can longer progress further in being administered biomarker tests. This means that the patient has converted from MCI to AD or the patient has not converted to AD and is recognized as the state, NAD. Patients recognized as AD or NAD no longer are administered biomarker tests and are no longer studied further in the Markov Chain. The transient states, those that are not absorbing states are patients that are recognized as being in an Inconclusive (I) state. These patients fall within an Inconclusive diagnosis once administered a biomarker test or more than one biomarker test. The Markov Chain is completed when all three tests are administered. There is a total of 36 states that have transition probabilities. Each transition probability must be multiplied by the assumption that the doctor randomly administers a biomarker test. The following matrix shows the highlighted 36 states. These 36 states represent transition probabilities, "p", and the probabilities of randomly administering a biomarker test being multiplied.

Current / Past	[0,0,0, I]	[1,0,0, AD]	[0,1,0, AD]	[0,0,1, AD]	[1,0,0, NAD]	[0,0,1, NAD]	[0,1,0, NAD]	[1,0,0, I]	[1,1,0, AD]	[1,0,1, AD]	[1,1,0, NAD]	[1,0,1, NAD]	[0,1,0, I]	[0,1,1, AD]	[0,1,1, NAD]	[0,0,1, I]	[1,1,0, I]	[1,0,1, I]	[0,1,1, I]	[1,1,1, AD]	[1,1,1, NAD]	[1,1,1,I]
[0,0,0, I]	1	p * (1/3)	p * (1/3)	p * (1/3)	p * (1/3)	p * (1/3)	p * (1/3)	p * (1/3)	0	0	0	0	p * (1/3)	0	0	p * (1/3)	0	0	0	0	0	0
[1,0,0, AD]	0	1	0	0	0	0	0	0	0	0	0	0	0	0	0	0	0	0	0	0	0	0
[0,1,0, AD]	0	0	1	0	0	0	0	0	0	0	0	0	0	0	0	0	0	0	0	0	0	0
[0,0,1, AD]	0	0	0	1	0	0	0	0	0	0	0	0	0	0	0	0	0	0	0	0	0	0
[1,0,0, NAD]	0	0	0	0	1	0	0	0	0	0	0	0	0	0	0	0	0	0	0	0	0	0
[0,0,1, NAD]	0	0	0	0	0	1	0	0	0	0	0	0	0	0	0	0	0	0	0	0	0	0
[0,1,0, NAD]	0	0	0	0	0	0	1	0	0	0	0	0	0	0	0	0	0	0	0	0	0	0
[1,0,0, I]	0	0	0	0	0	0	0	0	p * (1/2)	p * (1/2)	p * (1/2)	p * (1/2)	0	0	0	0	p * (1/2)	p * (1/2)	0	0	0	0
[1,1,0, AD]	0	0	0	0	0	0	0	0	1	0	0	0	0	0	0	0	0	0	0	0	0	0
[1,0,1, AD]	0	0	0	0	0	0	0	0	0	1	0	0	0	0	0	0	0	0	0	0	0	0
[1,1,0, NAD]	0	0	0	0	0	0	0	0	0	0	1	0	0	0	0	0	0	0	0	0	0	0
[1,0,1, NAD]	0	0	0	0	0	0	0	0	0	0	0	1	0	0	0	0	0	0	0	0	0	0
[0,1,0, I]	0	0	0	0	0	0	0	0	p * (1/2)	0	p * (1/2)	0	0	p * (1/2)	p * (1/2)	0	p * (1/2)	0	p * (1/2)	0	0	0
[0,1,1, AD]	0	0	0	0	0	0	0	0	0	0	0	0	0	1	0	0	0	0	0	0	0	0
[0,1,1, NAD]	0	0	0	0	0	0	0	0	0	0	0	0	0	0	1	0	0	0	0	0	0	0
[0,0,1, I]	0	0	0	0	0	0	0	0	p * (1/2)	0	p * (1/2)	0	p * (1/2)	p * (1/2)	0	0	p * (1/2)	p * (1/2)	0	0	0	0
[1,1,0, I]	0	0	0	0	0	0	0	0	0	0	0	0	0	0	0	0	0	0	0	p * (1)	p * (1)	p * (1)
[1,0,1, I]	0	0	0	0	0	0	0	0	0	0	0	0	0	0	0	0	0	0	0	p * (1)	p * (1)	p * (1)
[0,1,1, I]	0	0	0	0	0	0	0	0	0	0	0	0	0	0	0	0	0	0	0	p * (1)	p * (1)	p * (1)
[1,1,1, AD]	0	0	0	0	0	0	0	0	0	0	0	0	0	0	0	0	0	0	0	1	0	0
[1,1,1, NAD]	0	0	0	0	0	0	0	0	0	0	0	0	0	0	0	0	0	0	0	0	1	0
[1,1,1,I]	0	0	0	0	0	0	0	0	0	0	0	0	0	0	0	0	0	0	0	0	0	1

Figure 5: Transition Matrix of Markov Chain Model

The calculation of these transition probabilities will be discussed further in 3.4.1.d as well as the results. In addition, to formulating a transition matrix, a transition diagram also can be created to visually see the possible paths that a patient will undergo as the patient visits their doctor and is given a biomarker test.

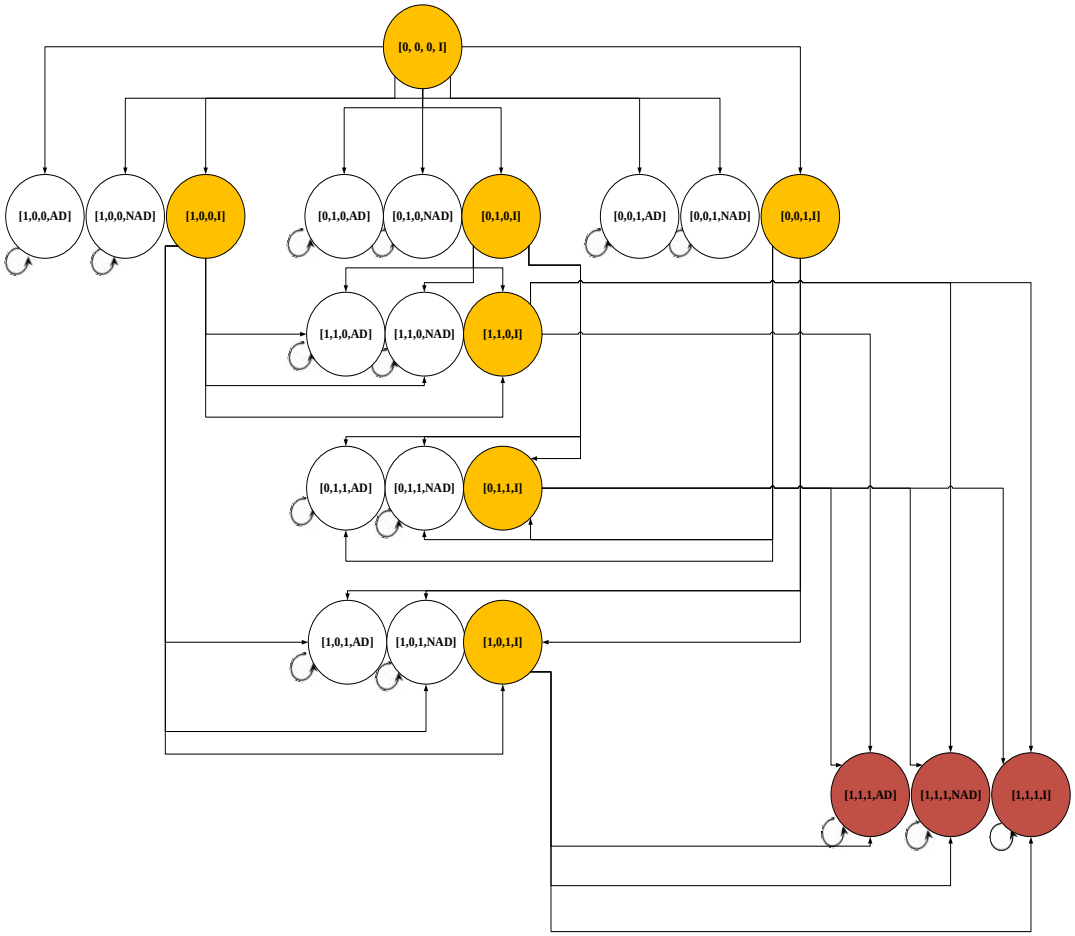

Figure 6: Transition Diagram of Markov Chain Model

The golden highlighted states in Figure 6 represent the transient states as these states are Inconclusive patients (I). The absorbing states are pictured as the states with recurring arrows and the red highlighted states are the conclusive states of the Markov Chain model. The conclusive states are all the possible three states: AD, NAD, I, once all tests have been administered.

3.4 Estimation of Markov Chain Components

3.4.1 Estimation Techniques Introduction

Different approaches were applied in the attempt to calculate the transition probabilities. The first necessary step was to normalize the data. This allowed the calculation of probabilities to be easier. The first attempt to calculate the transition probabilities was to use the method of input modeling, however this had its limitations and will be discussed further in section 3.4.1.c. The next plausible and selected method was to solve the transition probabilities by utilizing Empirical Cumulative Distribution Functions.

3.4.1.a Data Normalization

The calculation of these transition probabilities is important to understand the impact of the sequential sequence of biomarker test administration. Prior to calculating these probabilities with the original data explained in section 3.3, the data must be normalized. This is because the ranges of these biomarker tests must be taken into consideration as the p-Tau, FDG-PET, and Hippo tests all have different test values and ranges. The p-Tau test's values range from a minimum of 14 to a maximum of 171, the FDG-PET test's values range from a minimum of 0.88 to a maximum of 1.60, and the Hippo test's values range from a minimum of 1941 to a maximum of 4807. These test values must be normalized to adhere to different ranges. This normalization of the data is important for determining the joint density functions due to the combination of administered tests. The statistical software R was used to normalize this data from 0 to 1.

3.4.1.b Bayes' Formulation

The Markov Chain transition probabilities will be estimated using Bayesian methods. These Bayesian methods will help correspond the data with the current Markov Chain model. Bayes' theorem is made up from a posterior probability and a prior probability [17]. Bayes' theorem interchanges conditioning and updates based upon new information. One example from an absorption state such as [1, 1, 0, AD] states that the patient was administered the p-Tau and FDG-PET test and resulted in converting from MCI to AD. This specific state, [1, 1, 0, AD] is represented in the following Bayes' formulation:

$$P(AD \mid ptau, FDGpet) = \frac{P(ptau, FDGpet \mid AD) * P(AD)}{P(ptau, FDGpet)} \quad (4)$$

$P(AD \mid ptau, FDGpet)$ represents the posterior probability, where this is what occurs after both tests have been administered. $P(ptau, FDGpet \mid AD)$ represents the likelihood that given that the patient converted to contracting Alzheimer's Disease from being in an Inconclusive state, it calculates what the chance of that occurring due to being administered the p-Tau test and the FDG-PET test. The prior probability, $P(AD)$ is what occurs before tests have been administered. The evidence of this formula is $P(ptau, FDGpet)$ because it is known that these tests were administered.

3.4.1.c Input Modeling

Input models identify probability distributions from collected data. These probability distributions are determined from histograms. Histograms for continuous data such as the data in this research, correspond to the probability density function (PDF) of a theoretical distribution [11]. A line is drawn in the center of the bars of the histograms for

each interval based upon its frequency [11]. From these PDFs the calculation of probabilities could be calculated by using the parameters of these distributions, which includes the mean and standard deviation [11]. Software such as JMP allows users to input interested data into the software and a PDF and its parameters are provided. In this research, JMP was initially used to determine the PDFs of marginal densities and the PDFs of all tests individually. The following tables are examples of PDFs for the absorption state, [1, 1, 0, AD].

Marginal Density of FDG-PET: $f_{FDGPET\mid AD}$		
Type of Distribution	**PDF Graph**	**Parameters**
Normal	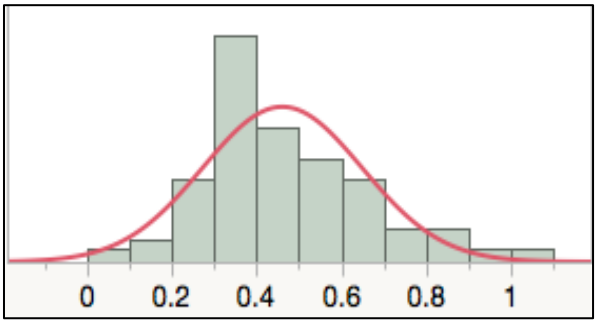	Mean = 0.460 Standard Deviation = 0.189

Table 2: Marginal Density of FDG-PET|AD

Marginal Density of p-Tau: $f_{ptau\mid AD}$		
Type of Distribution	**PDF Graph**	**Parameters**
Exponential	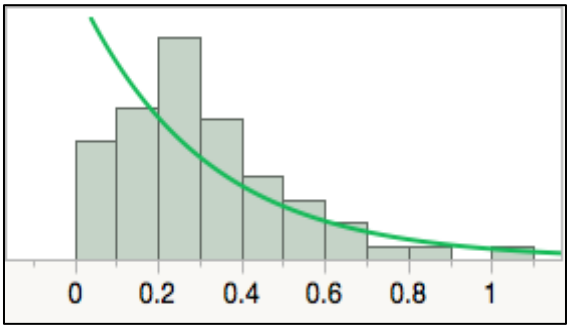	Standard Deviation = 0.305

Table 3: Marginal Density of p-Tau|AD

Density of FDG-PET: f_{FDGPET}		
Type of Distribution	**PDF Graph**	**Parameters**
Normal	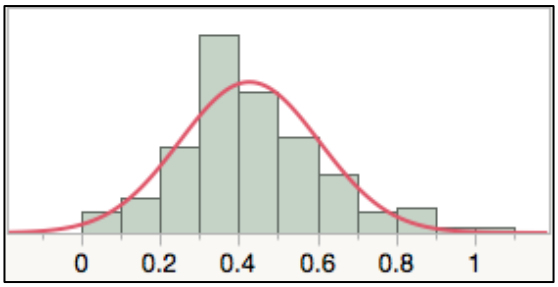	Mean = 0.427 Standard Deviation = 0.178

Table 4: Density of FDG-PET

Density of p-Tau: f_{p-Tau}		
Type of Distribution	**PDF Graph**	**Parameters**
Exponential	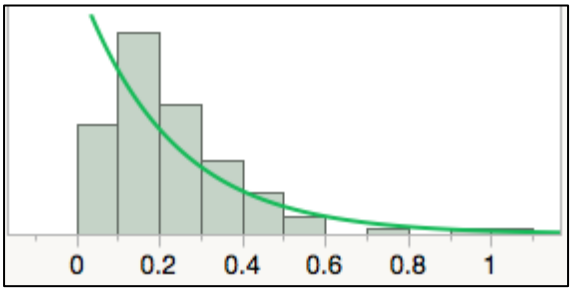	Standard Deviation = 0.224

Table 5: Density of p-Tau

Unfortunately, this method could not be conducted further because joint variables cannot be analyzed using JMP. The posterior probability illustrated in equation 4, $P(AD\ |ptau, FDGpet)$ could not be analyzed, nor provided a PDF and its parameters.

3.4.1.d Conditional Probabilities

In this research, it is important to understand the relationship between two and three random variables. These random variables represent the values of the biomarker tests. Due to the lack of an input modeling software that can provide the joint PDF of two and more

continuous random variables, the conditional probability will be utilized. The formation of a conditional probability will aid in determining the joint probability, $f_{X,Y}(x, y)$:

$$f_{X|Y}(x) = \frac{f_{X,Y}(x,y)}{f_Y(y)} \quad (5)$$

For example, equation 5 states the interest of determining the probability of X given Y is the joint probability of X and Y over the marginalized probability of Y. In this research, equation 5 is used to help calculate the probability of an example of transitioning from state [1, 0, 0, I] to [1, 1, 0, AD]. These two states mean that a patient is transitioning from a state of Inconclusive once given the p-Tau test, to a state of converting to AD after being given the FDG-PET test next.

3.4.1.e Empirical Cumulative Distribution Function (ECDF)

Before illustrating an example of a calculation of transition probabilities the thresholds of the three tests must be established as these thresholds determined when a patient would convert to AD, NAD, or I. Thresholds are established because probabilities are calculated by counting the number of patients below, above, or in between the thresholds. These counts illustrate the approach of utilizing Empirical Cumulative Distribution Functions (ECDF). ECDFs resample from the data collected and are used when there are no suitable theoretical distributions [11]. Since there are no viable theoretical distributions from input modeling due to joint variables, ECDFs illustrate the best option in calculating the transition probabilities.

The thresholds established for each biomarker were calculated by using the normalized test value data. The thresholds included upper bounds and lower bounds. These

bounds were calculated by determining the 25% quantile and 75% quantile of all test values for each test. The quantiles' values were calculated using R software. The p-Tau's upper bound is 0.2951 and the lower bound is 0.1183. If a data record represented a p-Tau test value of 0.2951 or above, then that patient converts to AD and if a p-Tau test value that is equal or less than 0.1183 does not convert to AD and is assigned as a state of NAD. A p-Tau test value that falls between the lower bound and upper bound values results in an Inconclusive (I) state. The FDG-PET's upper bound is 0.5266 and FDG-PET test values that are equal to or greater do not have AD and are assigned as a state of NAD. The lower bound of the FDG-PET is 0.3237 and test values that are equal to or less are assigned a state of AD. Test values between the upper bound and lower bound values are assigned a state of Inconclusive (I). The Hippo's upper bound is 0.5456 and test values that are equal and greater than are assigned a state of NAD and do not convert to AD. The lower bound of the Hippo test is 0.3235 and test values that are equal and less than are assigned a state of AD and converts AD. Test values that are between the upper bound and lower bound values are assigned a state of Inconclusive (I). Tables 6, 7, and 8 represent the summaries of the thresholds and patient state outcomes.

Test	**Normalized Data**	
p-Tau	**Thresholds**	**Outcome**
	≥ 0.2951Upper Bound	AD
	≤ 0.1183Lower Bound	NAD
	(0.1183, 0.2951)	I

Table 6: p-Tau Thresholds and Outcomes

Test	**Normalized Data**	
FDG-PET	**Thresholds**	**Outcome**
	≥ 0.5266Upper Bound	NAD
	≤ 0.3237Lower Bound	AD
	(0.3237, 0.5266)	I

Table 7: FDG-PET Thresholds and Outcomes

Test	Normalized Data	
	Thresholds	**Outcome**
Hippo	$\geq$ 0.5456Upper Bound	NAD
	$\leq$ 0.3235Lower Bound	AD
	(0.3235, 0.5456)	I

Table 8: Hippo Thresholds and Outcomes

After calculating these thresholds and determining the corresponding outcomes the collected data for each test was organized in a total of 13 intervals and each interval's width was $1/12$. These number of intervals and interval widths were decided upon the basis of constructing a histogram. Justification for following the basis of the construction of a histogram is because histograms are known as a frequency distribution charts and since ECDFs were the best option in determining transition probabilities, this organization of data would allow the feasibility of counts. The number of intervals, 13, for each test was determined by using the rule of thumb in constructing histograms, where the number of intervals is the square root of the total number of data records [12]. Since there is a total of 144 data records the square root of 144 is 12, however the interval width is the best when it is equal as possible and the interval width was calculated by inverting 12 to equal $1/12 = 0.0833$ and by adding each interval width it equated to a total 13 equal width intervals [12]. Table 9 serves as an example of the intervals for each test.

Intervals	Bins
1	0-0.0833
2	0.0833-0.1666
3	0.1666-0.2499
4	0.2499-0.3332
5	0.3332-0.4165
6	0.4165-0.4998
7	0.4998-0.5831
8	0.5831-0.6664
9	0.6664-0.7497
10	0.7497-0.833
11	0.833-0.9163
12	0.9163-0.9996
13	0.9996-1

Table 9: Intervals for Each Test

An example of utilizing the ECDF approach, is as follows, where the interest is calculating the probability of transitioning to state [1, 1, 0, AD]. This state means that both the p-Tau and the FDG-PET test were administered to this patient and this patient converted to obtaining AD. This interested resultant state has two possible past states: [0, 1, 0, I] and [1, 0, 0, I], where the patient could have first been given the FDG-PET test and resulted in an Inconclusive test status or the patient could have been first given the p-Tau test and resulted in an Inconclusive test status. The ECDF of a p-Tau test and FDG-PET test is shown in Figure 7.

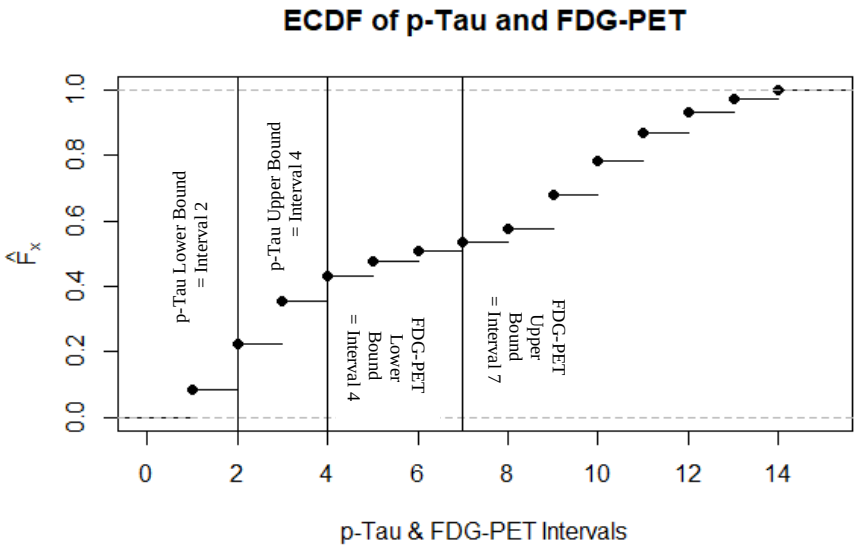

Figure 7: ECDF Graph of p-Tau and FDG-PET tests

The X-axis represents the intervals associated to the corresponding test values. The p-Tau lower bound corresponds to interval 2 and the upper bound interval of p-Tau is 4. The FDG-PET lower bound corresponds to interval 4 and the upper bound interval of FDG-PET is 7. The corresponding intervals contains the 25% and 75% quantile values. These intervals are determined by referencing Table 9.

From these corresponding intervals the probabilities were calculated by the following equations that utilize the conditional probabilities of the previous states.

$$P_{pTau}(pTau \geq pTau^{UB} \mid FDGpet \in [FDGpet^{UB}, FDGpet^{LB}]) * P(choose\ pTau\ test\ randomly = 1/2) \quad (6)$$

$$P_{FDGpet}(FDGpet \leq FDGpet^{LB} \mid pTau \in [pTau^{UB}, pTau^{LB}]) * P(choose\ FDGpet\ test\ randomly = 1/2) \quad (7)$$

Equation 6 references the probability of being administered the FDG-PET next after initially being administered the p-Tau test. Equation 7 references the probability of being administered the p-Tau test next after initially being administered the FDG-PET test. The notation UB and LB are abbreviated respectively for upper bound and lower bound.

Equation 6 states that the probability that the test, p-Tau is administered after FDG-PET is when the test value is equal to or greater than the upper bound of p-Tau and that is when the test value is equal to or greater than 0.2951 and this is when the corresponding interval is 2. Therefore, the probability of this transition is calculated by counting all the test value instances of p-Tau that are greater than interval 2 when the FDG-PET is in the state of Inconclusive and that occurs when the test value is between the lower bound and upper bound of FDG-PET, (0.3237, 0.5266) which equates to the intervals 5 and 6 which are between the lower bound interval 4 and upper bound interval 7. Then that count is divided by the sum of all p-Tau test values within that Inconclusive state interval of FDG-PET and that equals the transition probability. That transition probability is then multiplied by the random assumption probability that the biomarker tests are randomly chosen. Equation 7 follows the same suit, however with the switched condition variable of p-Tau. The following table shows the respective transition probabilities for equations 6 and 7.

Equation	Past State	Current State	Transition Probability
6	[0, 1, 0, I]	[1, 1, 0, AD]	14%
7	[1, 0, 0, I]	[1, 1, 0, AD]	19%

Table 10: Two Different Transition Probabilities for p-Tau and FDG-PET Tests

3.4.2 Results Introduction

From utilizing the ECDF approach, the following sections demonstrate the results of the calculations of all the possible transition probabilities for each feasible transition. The absorption probabilities of the absorbing states of the Markov Chain are further calculated and shown by the utilization of reordering the transition matrix of the position of transient probabilities and the position of the probabilities from transient to absorbing states, adding a submatrix of zero entries, and adding the submatrix of an identity matrix [13].

3.4.2.a Transition Probabilities

The following figure represents the calculations of all the transition probabilities of transient and absorption states. All calculations were conducted using Excel, specifically Pivot Tables, and nested functions.

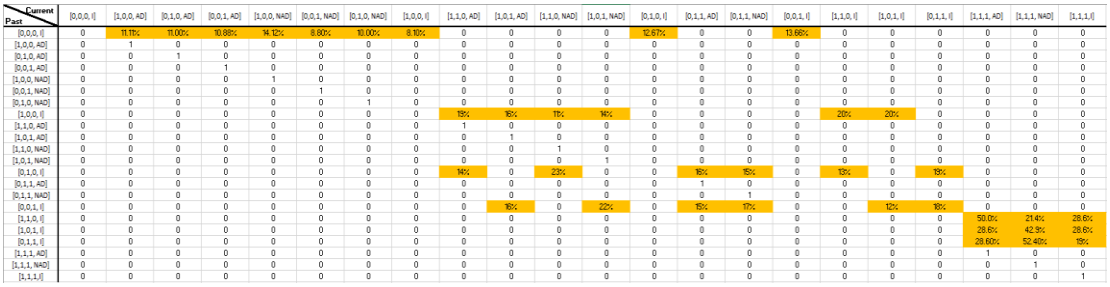

Figure 8: Transition Matrix Results

These transition probabilities of this Markov Chain are verified and confirmed as each row sums up to 1. As shown in Figure 5, the transition matrix framework, the same 36 probabilities are calculated and are highlighted.

3.4.2.b Markov Chain Calculations

The Markov Chain being modeled is classified as an absorbing Markov Chain because it contains both transient and absorbing states [13]. There is interest in the absorbing chain because there are inquires of:

1) What is the probability that a patient will end up in an absorbing state given that the patient started in a specific transient state? [15].
2) How many expected time periods does a patient spend in a transient state before the patient reaches an absorption state? [15].

The created transition matrix shown in Figure 8, is reorganized by classes of states by the following organization and notation:

P =	s – m columns (Transient States)	m columns (Absorbing States)
s – m rows (Transient States)	**Q**	**R**
m rows (Absorbing States)	**0**	**I**

Table 11: Reorganization of Transition Matrix Framework

The notations are as follows, P corresponds to the transition matrix in Figure 8, s = number of states = 22, and m = number of absorbing states = 15, **Q =** Transient State Probabilities, **R =** Absorbing State Probabilities, **0 =** Submatrix of zero elements, **I =** Identity Matrix [14, 15]. The reorganized matrix represented in Figure 9, helps answer the first and second inquiry mentioned previously. The reorganized matrix and the following

equations were calculated using MATLAB. The first inquiry is calculated with equation 8 and the second inquiry is calculated with equation 9.

$$(I - Q)^{-1} * R \tag{8}$$

$$(I - Q)^{-1} \tag{9}$$

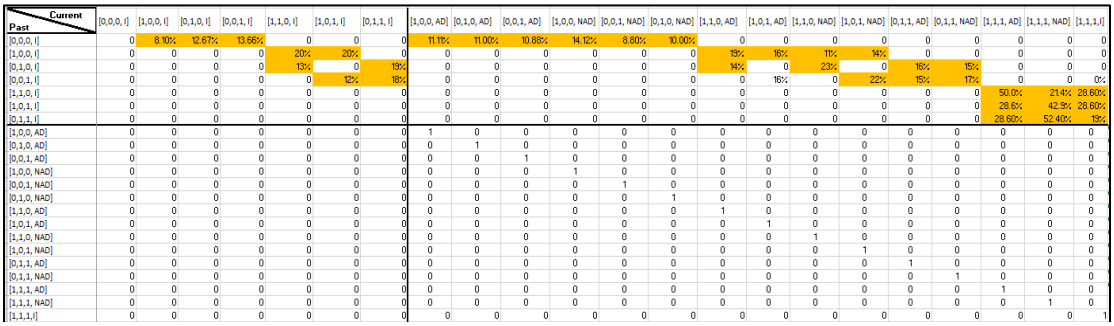

Past \ Current	[0,0,0, I]	[1,0,0, I]	[0,1,0, I]	[0,0,1, I]	[1,1,0, I]	[1,0,1, I]	[0,1,1, I]	[1,0,0, AD]	[0,1,0, AD]	[0,0,1, AD]	[1,0,0, NAD]	[0,0,1, NAD]	[0,1,0, NAD]	[1,1,0, AD]	[1,0,1, AD]	[1,1,0, NAD]	[1,0,1, NAD]	[0,1,1, AD]	[0,1,1, NAD]	[1,1,1, AD]	[1,1,1, NAD]	[1,1,1,I]
[0,0,0, I]	0	8.10%	12.67%	13.66%	0	0	0	11.11%	11.00%	10.88%	14.12%	8.80%	10.00%	0	0	0	0	0	0	0	0	0
[1,0,0, I]	0	0	0	0	20%	20%	0	0	0	0	0	0	0	19%	16%	11%	14%	0	0	0	0	0
[0,1,0, I]	0	0	0	0	13%	0	13%	0	0	0	0	0	0	14%	0	23%	0	16%	15%	0	0	0
[0,0,1, I]	0	0	0	0	0	12%	18%	0	0	0	0	0	0	0	16%	0	22%	15%	17%	0	0	0%
[1,1,0, I]	0	0	0	0	0	0	0	0	0	0	0	0	0	0	0	0	0	0	0	50.0%	21.4%	28.60%
[1,0,1, I]	0	0	0	0	0	0	0	0	0	0	0	0	0	0	0	0	0	0	0	28.6%	42.9%	28.60%
[0,1,1, I]	0	0	0	0	0	0	0	0	0	0	0	0	0	0	0	0	0	0	0	28.60%	52.40%	19%
[1,0,0, AD]	0	0	0	0	0	0	0	1	0	0	0	0	0	0	0	0	0	0	0	0	0	0
[0,1,0, AD]	0	0	0	0	0	0	0	0	1	0	0	0	0	0	0	0	0	0	0	0	0	0
[0,0,1, AD]	0	0	0	0	0	0	0	0	0	1	0	0	0	0	0	0	0	0	0	0	0	0
[1,0,0, NAD]	0	0	0	0	0	0	0	0	0	0	1	0	0	0	0	0	0	0	0	0	0	0
[0,0,1, NAD]	0	0	0	0	0	0	0	0	0	0	0	1	0	0	0	0	0	0	0	0	0	0
[0,1,0, NAD]	0	0	0	0	0	0	0	0	0	0	0	0	1	0	0	0	0	0	0	0	0	0
[1,1,0, AD]	0	0	0	0	0	0	0	0	0	0	0	0	0	1	0	0	0	0	0	0	0	0
[1,0,1, AD]	0	0	0	0	0	0	0	0	0	0	0	0	0	0	1	0	0	0	0	0	0	0
[1,1,0, NAD]	0	0	0	0	0	0	0	0	0	0	0	0	0	0	0	1	0	0	0	0	0	0
[1,0,1, NAD]	0	0	0	0	0	0	0	0	0	0	0	0	0	0	0	0	1	0	0	0	0	0
[0,1,1, AD]	0	0	0	0	0	0	0	0	0	0	0	0	0	0	0	0	0	1	0	0	0	0
[0,1,1, NAD]	0	0	0	0	0	0	0	0	0	0	0	0	0	0	0	0	0	0	1	0	0	0
[1,1,1, AD]	0	0	0	0	0	0	0	0	0	0	0	0	0	0	0	0	0	0	0	1	0	0
[1,1,1, NAD]	0	0	0	0	0	0	0	0	0	0	0	0	0	0	0	0	0	0	0	0	1	0
[1,1,1,I]	0	0	0	0	0	0	0	0	0	0	0	0	0	0	0	0	0	0	0	0	0	1

Figure 9: Reorganized Transition Matrix

Additionally, the transient states and absorption states are outlined in Table 12.

Transient States		**Absorbent States**	
[0, 0, 0, I]	[1, 0, 0, I]	[1, 0, 0, AD]	[0, 1, 0, AD]
[0, 1, 0, I]	[0, 0, 0, I]	[0, 0, 1, AD]	[1, 0, 0, NAD]
[1, 1, 0, I]	[1, 0, 1, I]	[0, 0, 1, NAD]	[0, 1, 0, NAD]
[0, 1, 1, I]		[1, 1, 0, AD]	[1, 0, 1, AD]
		[1, 1, 0, NAD]	[1, 0, 1, NAD]
		[0, 1, 1, AD]	[0, 1, 1, NAD]
		[1, 1, 1, AD]	[1, 1, 1, NAD]
		[1, 1, 1, I]	

Table 12: Transient and Absorbent States of Markov Chain

The probabilities for the first inquiry are represented in Figure 10 and the expected number of time periods for the second inquiry are represented in Figure 11.

Markov Chain Model Absorption Probabilities

	[1,0,0, AD]	[0,1,0, AD]	[0,0,1, AD]	[1,0,0, NAD]	[0,0,1, NAD]	[0,1,0, NAD]	[1,1,0, AD]	[1,0,1, AD]	[1,1,0, NAD]	[1,0,1, NAD]	[0,1,1, AD]	[0,1,1, NAD]	[1,1,1, AD]	[1,1,1, NAD]	[1,1,1,I]
[0,0,0, I]	0.1111	0.11	0.1088	0.1412	0.088	0.1	0.033128	0.034816	0.038051	0.041392	0.040762	0.042227	0.039573858	0.046471926	0.027910808
[1,0,0, I]	0	0	0	0	0	0	0.19	0.16	0.11	0.14	0	0	0.1572	0.1286	0.1144
[0,1,0, I]	0	0	0	0	0	0	0.14	0	0.23	0	0.16	0.15	0.11934	0.12738	0.07328
[0,0,1, I]	0	0	0	0	0	0	0	0.16	0	0.22	0.15	0.17	0.0858	0.1458	0.06852
[1,1,0, I]	0	0	0	0	0	0	0	0	0	0	0	0	0.5	0.214	0.286
[1,0,1, I]	0	0	0	0	0	0	0	0	0	0	0	0	0.286	0.429	0.286
[0,1,1, I]	0	0	0	0	0	0	0	0	0	0	0	0	0.286	0.524	0.19

Figure 10: Markov Chain Model Absorption Probabilities

Expected Time

	[0,0,0, I]	[1,0,0, I]	[0,1,0, I]	[0,0,1, I]	[1,1,0, I]	[1,0,1, I]	[0,1,1, I]
[0,0,0, I]	1	0.081	0.1267	0.1366	0.032671	0.032592	0.048661
[1,0,0, I]	0	1	0	0	0.2	0.2	0
[0,1,0, I]	0	0	1	0	0.13	0	0.19
[0,0,1, I]	0	0	0	1	0	0.12	0.18
[1,1,0, I]	0	0	0	0	1	0	0
[1,0,1, I]	0	0	0	0	0	1	0
[0,1,1, I]	0	0	0	0	0	0	1

Figure 11: Expected # of Time Periods in Transient State Prior to Absorption

The absorption probabilities in Figure 10 follow a trend that as more tests are administered there is a higher likelihood of a patient not contracting AD. An example interpretation of Figure 11, states that starting at state [0, 0, 0, I] will result in the expected number of time periods that a patient stays in state [0, 0, 0, I] is 1, the expected number of time periods a patient stays in state [1, 0, 0, I] is 0.081, and so forth.

CHAPTER 4: NUMERICAL RESULTS

4.1 Introduction

As with any type of model formulation, it is best practice to validate and verify the model. Model validation encompasses the interaction between the real system, which is the research problem of optimizing the biomarker test administration policy decisions that improve the accuracy in detecting patients that will contract Alzheimer's Disease and those who do not, to the Markov Chain model of that system [11]. This interaction can be

validated with the verification of the Markov Chain model to a simulation of the model. The Markov Chain model can be verified by producing simulations of all possible transitions from transient states to absorbent states. Simulations of the Markov Chain model will show the impact of the lower bound and upper bound thresholds. As stated previously in this paper, the thresholds determine the likelihood of a patient contracting AD or not. The simulations of the Markov Chain model are conducted by a coded simulation. The simulation code is explained in the following section.

4.1.1 Simulation Background

Simulation code was created using MATLAB. This simulation code runs 1,000 replications of modeling sample paths from transient states to the absorbent states. The input of the transition matrix shown in Figure 9 and the initial transient state must be manually executed in the MATLAB code. The sample paths from these replications are then used to calculate the absorbing probabilities.

4.1.2 Markov Chain Model Verification

The initial absorption probabilities from the Markov Chain model shown in Figure 10 must be compared to the calculated absorption probabilities from the simulation model. The Markov Chain model can only be verified if there is no difference between the Markov Chain absorption probabilities and simulation model absorption probabilities. This verification step involves a similar procedure conducted in section 3.4.1.e, when transition probabilities were empirically calculated. The simulation code produced all the possible states that could be reached from a starting state of a transient state. Table 13 is an example

of the possible transition paths for the initial state, [0, 0, 0, I]. Table 14 serves as a reference to associate each numerical state from the simulation to the corresponding vector state.

# of Reps	Initial State	State 1	State 2	State 3
1	1	13	0	0
2	1	4	19	0
3	1	13	0	0
4	1	12	0	0
5	1	10	0	0
…	…	…	…	…
996	1	10	0	0
997	1	12	0	0
998	1	9	0	0
999	1	3	5	20
1000	1	11	0	0

Table 13: Sample Transition Path from Simulation Code

Transient States		Absorbent States		Absorbent States	
Simulation State	Vector State	Simulation State	Vector State	Simulation State	Vector State
1	[0,0,0, I]	8	[1,0,0, AD]	15	[1,0,1, AD]
2	[1,0,0, I]	9	[0,1,0, AD]	16	[1,1,0, NAD]
3	[0,1,0, I]	10	[0,0,1, AD]	17	[1,0,1, NAD]
4	[0,0,1, I]	11	[1,0,0, NAD]	18	[0,1,1, AD]
5	[1,1,0, I]	12	[0,0,1, NAD]	19	[0,1,1, NAD]
6	[1,0,1, I]	13	[0,1,0, NAD]	20	[1,1,1, AD]
7	[0,1,1, I]	14	[1,1,0, AD]	21	[1,1,1, NAD]
				22	[1,1,1,I]

Table 14: State Reference

From Table 13, each time an absorbent state, identified as 8-22 was listed, the count was summed for each absorbent state and divided by the total number of repetitions conducted from the simulation which was 1,000. The following equation is the equation used to calculate each probability in Figure 12.

$$\frac{total\ count\ of\ absorbtion\ state\ visted}{1{,}000} \tag{10}$$

Simulation Absorption Probabilities															
	[1,0,0, AD]	[0,1,0, AD]	[0,0,1, AD]	[1,0,0, NAD]	[0,0,1, NAD]	[0,1,0, NAD]	[1,1,0, AD]	[1,0,1, AD]	[1,1,0, NAD]	[1,0,1, NAD]	[0,1,1, AD]	[0,1,1, NAD]	[1,1,1, AD]	[1,1,1, NAD]	[1,1,1,I]
[0,0,0, I]	0.097	0.111	0.095	0.158	0.078	0.111	0.029	0.033	0.049	0.042	0.046	0.039	0.036	0.045	0.031
[1,0,0, I]	0	0	0	0	0	0	0.185	0.145	0.117	0.154	0	0	0.144	0.131	0.124
[0,1,0, I]	0	0	0	0	0	0	0.132	0	0.207	0	0.178	0.166	0.106	0.132	0.079
[0,0,1, I]	0	0	0	0	0	0	0	0.152	0	0.195	0.163	0.197	0.082	0.138	0.073
[1,1,0, I]	0	0	0	0	0	0	0	0	0	0	0	0	0.489	0.2	0.311
[1,0,1, I]	0	0	0	0	0	0	0	0	0	0	0	0	0.286	0.404	0.31
[0,1,1, I]	0	0	0	0	0	0	0	0	0	0	0	0	0.286	0.502	0.212

Figure 12: Calculated Simulation Absorption Probabilities

Figure 10, the Markov Chain model absorption probabilities and Figure 12, the simulation model's absorption probabilities are then statistically compared by conducting a F-test. A F-test tests the hypothesis on the equality of the variances of two different data sets [16]. Equation 11 illustrates the null (H_0) and alternate (H_a) hypothesis being tested.

$$H_0: \sigma_1^2 = \sigma_2^2$$
$$H_a: \sigma_1^2 \neq \sigma_2^2 \tag{11}$$

This states that if the variance within the Markov Chain model absorption probabilities and the variance within the simulation model absorption probabilities are not statistically significant the two sets of absorption probabilities are essentially the same. Table 15 contains the F-test results:

	Markov Chain Model	*Simulation Model*
Mean	0.066711929	0.066666667
Variance	0.011544883	0.011299186
Observations	105	105
df	104	104
F	1.021744659	
P(F<=f) one-tail	0.456433199	
F Critical one-tail	1.382732799	

Table 15: F-test Results

Since the F statistic, 1.02 is smaller than the F critical value, 1.38, the null hypothesis, H_0 is not rejected. This means that the two data sets' variances are equal. This verifies that the simulation model and the Markov Chain model do no differ. This proves that the Markov Chain can effectively model different types of parameter changes that are conducted in the following section.

4.2 Experiments

The parameter changes for this Markov Chain model are conducted by simulating different experiments. Two types of experiments are demonstrated. The first experiment is the tightening of the AD classification thresholds. The thresholds mentioned in tables 6, 7, and 8 are the values that determine the patients' classification of contracting AD or not. The second experiment involves testing all possible biomarker test sequences. Both experiments were decided upon because both are two main parameter inputs in simulating the Markov Chain.

These experiments were conducted to demonstrate the impact the thresholds and specified test sequences can have on the probability of patients contracting AD and the expected time spent in transient states before absorption. Simulations of these experiments of the Markov Chain model provide evidence that the Markov Chain can efficiently model different parameters of the evolution of MCI patients. The Markov Chain is a more complex model than the STC model and these simulations demonstrate that the Markov Chain model can replace the STC model due to its capability of simulating complex parameters.

4.2.1 Tightening AD Threshold

The F-test results verified the ability of the Markov Chain to model different parameters of the thresholds. The thresholds that classify patients as converting to AD was tightened. The threshold for the p-Tau test was changed from representing the 75% quantile to tightening it to the 65% quantile. The AD conversion threshold for the FDG-PET test changed from the 25% quantile to the 35% quantile. The Hippo test's threshold for AD conversion changed from the 25% quantile to the 35% quantile. The highlighted data values changed accordingly:

Test	**Normalized Data**	
	Thresholds	**Outcome**
p-Tau	≥ 0.23971Upper Bound	AD
	≤ 0.1183Lower Bound	NAD
	(0.1183, 0.2951)	I

Table 16: p-Tau Thresholds and Outcomes

Test	**Normalized Data**	
	Thresholds	**Outcome**
FDG-PET	≥ 0.5266Upper Bound	NAD
	≤ 0.3466Lower Bound	AD
	(0.3237, 0.5266)	I

Table 17: FDG-PET Thresholds and Outcomes

Test	**Normalized Data**	
	Thresholds	**Outcome**
Hippo	≥ 0.5456Upper Bound	NAD
	≤ 0.3627Lower Bound	AD
	(0.3235, 0.5456)	I

Table 18: Hippo Thresholds and Outcomes

As demonstrated in Chapter 3, these threshold values correspond respectively to established numeric interval values in Table 9. These intervals aid in calculating the transition probabilities for the newly established AD thresholds. As demonstrated in the example in section 3.4.1.e, the transition probabilities are calculated in the same manner and are represented in the following transition matrix:

Current / Past	[0,0,0, I]	[1,0,0, AD]	[0,1,0, AD]	[0,0,1, AD]	[1,0,0, NAD]	[0,0,1, NAD]	[0,1,0, NAD]	[1,1,0, AD]	[1,0,1, AD]	[1,1,0, NAD]	[1,0,1, NAD]	[0,1,0, I]	[0,1,1, AD]	[0,1,1, NAD]	[0,0,1, I]	[1,1,0, I]	[1,0,1, I]	[0,1,1, I]	[1,1,1, AD]	[1,1,1, NAD]	[1,1,1,I]
[0,0,0, I]	0	19.21%	9.95%	10.88%	14.12%	16.90%	17.82%	0	0	0	0	5.56%	0	0	5.56%	0	0	0	0	0	0
[1,0,0, AD]	0	1	0	0	0	0	0	0	0	0	0	0	0	0	0	0	0	0	0	0	0
[0,1,0, AD]	0	0	1	0	0	0	0	0	0	0	0	0	0	0	0	0	0	0	0	0	0
[0,0,1, AD]	0	0	0	1	0	0	0	0	0	0	0	0	0	0	0	0	0	0	0	0	0
[1,0,0, NAD]	0	0	0	0	1	0	0	0	0	0	0	0	0	0	0	0	0	0	0	0	0
[0,0,1, NAD]	0	0	0	0	0	1	0	0	0	0	0	0	0	0	0	0	0	0	0	0	0
[0,1,0, NAD]	0	0	0	0	0	0	1	0	0	0	0	0	0	0	0	0	0	0	0	0	0
[1,1,0, AD]	0	0	0	0	0	0	0	1	0	0	0	0	0	0	0	0	0	0	0	0	0
[1,0,1, AD]	0	0	0	0	0	0	0	0	1	0	0	0	0	0	0	0	0	0	0	0	0
[1,1,0, NAD]	0	0	0	0	0	0	0	0	0	1	0	0	0	0	0	0	0	0	0	0	0
[1,0,1, NAD]	0	0	0	0	0	0	0	0	0	0	1	0	0	0	0	0	0	0	0	0	0
[0,1,0, I]	0	0	0	0	0	0	0	25.00%	0	25.00%	0	0	27%	8%	0	0	0	15%	0	0	0
[0,1,1, AD]	0	0	0	0	0	0	0	0	0	0	0	0	1	0	0	0	0	0	0	0	0
[0,1,1, NAD]	0	0	0	0	0	0	0	0	0	0	0	0	0	1	0	0	0	0	0	0	0
[0,0,1, I]	0	0	0	0	0	0	0	0	42%	0	2%	0	29%	13%	0	0	6%	8%	0	0	0
[1,1,0, I]	0	0	0	0	0	0	0	0	0	0	0	0	0	0	0	0	0	0	42%	23%	35%
[1,0,1, I]	0	0	0	0	0	0	0	0	0	0	0	0	0	0	0	0	0	0	47%	34%	19%
[0,1,1, I]	0	0	0	0	0	0	0	0	0	0	0	0	0	0	0	0	0	0	25%	75%	0%
[1,1,1, AD]	0	0	0	0	0	0	0	0	0	0	0	0	0	0	0	0	0	0	1	0	0
[1,1,1,	0	0	0	0	0	0	0	0	0	0	0	0	0	0	0	0	0	0	0	1	0
[1,1,1,I]	0	0	0	0	0	0	0	0	0	0	0	0	0	0	0	0	0	0	0	0	1

Figure 13: Transition Matrix for Adjusted AD Thresholds

The Markov Chain model absorption probabilities seen in Figure 14, were also calculated in the same manner using MATLAB as explained in section, 3.4.2.b.

Markov Chain Model Absorption Probabilities																
	[1,0,0, AD]	[0,1,0, AD]	[0,0,1, AD]	[1,0,0, NAD]	[0,0,1, NAD]	[0,1,0, NAD]	[1,1,0, AD]	[1,0,1, AD]	[1,1,0, NAD]	[1,0,1, NAD]	[0,1,1, AD]	[0,1,1, NAD]	[1,1,1, AD]	[1,1,1, NAD]	[1,1,1,I]
[0,0,0, I]	0.1921296	0.099537	0.1087963	0.1412037	0.1689815	0.1782407	0.0138889	0.0231481	0.0138889	0.0011574	0.03125	0.0115741	0.0048307	0.0107256	0.0006474
[0,1,0, I]	0	0	0	0	0	0	0.25	0	0.25	0	0.2708333	0.0833333	0.0364583	0.109375	0
[0,0,1, I]	0	0	0	0	0	0	0	0.4166667	0	0.0208333	0.2916667	0.125	0.0504944	0.0836864	0.0116525
[1,1,0, I]	0	0	0	0	0	0	0	0	0	0	0	0	0.4193548	0.2258065	0.3548387
[1,0,1, I]	0	0	0	0	0	0	0	0	0	0	0	0	0.4745763	0.3389831	0.1864407
[0,1,1, I]	0	0	0	0	0	0	0	0	0	0	0	0	0.25	0.75	0

Figure 14: Absorption Probabilities for Adjusted AD Threshold

The expected number of time periods spent in a transient state prior to entering an absorbent state is represented by Figure 15. These time periods were calculated by equation 9.

Expected Time						
	[0,0,0, I]	[0,1,0, I]	[0,0,1, I]	[1,1,0, I]	[1,0,1, I]	[0,1,1, I]
[0,0,0, I]	1	0.055556	0.055556	0	0.003472	0.012731
[0,1,0, I]	0	1	0	0	0	0.145833
[0,0,1, I]	0	0	1	0	0.0625	0.083333
[1,1,0, I]	0	0	0	1	0	0
[1,0,1, I]	0	0	0	0	1	0
[0,1,1, I]	0	0	0	0	0	1

Figure 15: Expected # of Time Periods in Transient State Before Absorption State from New AD Thresholds

4.2.1.a Experiment 1 Data Comparison

A comparison between the absorption probabilities of tightened AD thresholds and the original thresholds was conducted. A F-test resulted in a F statistic of 1.55 and F critical

value of 1.40. Since the F statistic is greater than the F critical value, this stated that there was statistically enough evidence to reject the null hypothesis that the variances between the two sets are the same. Comparing Figure 10 and Figure 14 side-by-side shows that Figure 14 has one less transient state than Figure 10. This is because due to a tighter AD threshold, the Inconclusive interval for p-Tau was non-existent and this resulted in zero visits to state, [1, 0, 0, I]. Therefore, because of the exclusion of this state, there is a significance difference among the original thresholds and new thresholds. Since, there were no possible visits to an Inconclusive state, it can be inferred that the new tighter AD thresholds will perform better in confidently classifying patient's conversions to attaining AD or not attaining AD. Additionally, there will be a subgroup of patients that will not need to be administered more biomarker tests and this would lead to a decrease of the cost of tests and time of diagnosis.

Another set of comparisons was conducted. The initial data from ADNI mentioned in section, 3.2, were compared against the absorption probabilities from Figure 14 and compared against the absorption probabilities provided in Figure 10. The total probability of patients that contracted AD and the total probability of patients that did not contract AD, denoted as NAD, were analyzed among these three data sets. The Inconclusive state, I, was not compared between all these 3 different data sets because the patient data set did not have information about patients that were classified as Inconclusive.

The patient data set classified that 50% patients contracted AD and the other 50% did not contract AD. Table 19 demonstrates the total probabilities of patients contracting AD and not contracting AD (NAD) from Figure 14 which represents the tightened AD

thresholds and from Figure 10 which represents the original thresholds. From the tightened AD thresholds there is a 2% differential of AD conversion and a 9% differential of NAD conversion from the patient data set. The original thresholds resulted in a 10% differential of AD conversion and a 6% differential of NAD conversion from the patient data set. These differentials make sense because the percentage of patients that contracted AD increased when the AD thresholds were tightened compared against the original thresholds. The tightening of the AD threshold allows more patients to be classified as AD patients. Nonetheless both sets of thresholds were within a 10% difference compared against the original patient classification.

Patient Data Set		**Tightened AD Thresholds (Figure 14)**		**Original Thresholds (Figure 10)**	
Outcome	Probability	Outcome	Probability	Outcome	Probability
AD	50%	AD	48%	AD	40%
NAD	50%	NAD	41%	NAD	44%

Table 19: Outcome Comparison

The expected time periods could not be compared against the provided data set because that information was not provided. Therefore, the comparison of the expected time periods spent in transient states before visiting absorption states were conducted for the tightened AD thresholds, seen in Figure 15 against the original thresholds seen in Figure 11. A F-test resulted in a F statistic of 1.30 and a F critical value of 1.67. Since the F statistic was smaller than the F critical value, this illustrates that variances between the two data sets are not significantly different and the expected number of time periods in the transient states between the two different thresholds are similar. The expected number of time

periods in transient states in Figures 11 and 15 never exceeded the time period of 1. The maximum time spent in a transient state was 0.19 of a time period.

4.2.2 Fixed Test Sequences

Further Markov Chain model analysis was conducted to illustrate the impact fixed test sequences had on absorption probabilities and the expected time periods spent in transient states. The three tests: p-Tau, FDG-PET, and Hippo have six possible sequences:

1) p-Tau → FDG-PET → Hippo
2) FDG-PET → p-Tau → Hippo
3) p-Tau → Hippo → FDG-PET
4) Hippo → p-Tau → FDG-PET
5) FDG-PET → Hippo → p-Tau
6) Hippo → FDG-PET → p-Tau

The following absorption probabilities are illustrated in Figure 16 for each fixed sequence above as well as the expected time spent in the transient states are illustrated in Figure 17. The transition matrixes for these six sequences equated to fewer amount of total states. The number of transient states for each test sequence was 3, while the number of absorbent states was 7.

Sequence #		[1,0,0, AD]	[1,0,0, NAD]	[1,1,0, AD]	[1,1,0, NAD]	[1,1,1, AD]	[1,1,1, NAD]	[1,1,1,I]
	[0,0,0, I]	0.342465753	0.417808219	0.089041096	0.054794521	0.030187722	0.028411974	0.037290715
1	[1,0,0, I]	0	0	0.371428571	0.228571429	0.125925926	0.118518518	0.155555556
	[1,1,0, I]	0	0	0	0	0.314814815	0.296296296	0.388888889
		[0,1,0, AD]	[0,1,0, NAD]	[1,1,0, AD]	[1,1,0, NAD]	[1,1,1, AD]	[1,1,1, NAD]	[1,1,1,I]
	[0,0,0, I]	0.326388889	0.298611111	0.104166667	0.173611111	0.030555555	0.027777778	0.038888889
2	[0,1,0, I]	0	0	0.277777778	0.462962963	0.081481481	0.074074074	0.103703704
	[1,1,0, I]	0	0	0	0	0.314285714	0.285714286	0.4
		[1,0,0, AD]	[1,0,0, NAD]	[1,0,1, AD]	[1,0,1, NAD]	[1,1,1, AD]	[1,1,1, NAD]	[1,1,1,I]
	[0,0,0, I]	0.333333333	0.423611111	0.076388889	0.069444445	0.029661017	0.032956686	0.03460452
3	[1,0,0, I]	0	0	0.314285714	0.285714286	0.122033898	0.13559322	0.142372881
	[1,0,1, I]	0	0	0	0	0.305084746	0.338983051	0.355932203
		[0,0,1, AD]	[0,0,1, NAD]	[1,0,1, AD]	[1,0,1, NAD]	[1,1,1, AD]	[1,1,1, NAD]	[1,1,1,I]
	[0,0,0, I]	0.263888889	0.326388889	0.131944444	0.180555555	0.036111111	0.022222222	0.038888889
4	[0,0,1, I]	0	0	0.322033898	0.440677966	0.088135593	0.054237288	0.094915254
	[1,0,1, I]	0	0	0	0	0.371428571	0.228571429	0.4
		[0,1,0, AD]	[0,1,0, NAD]	[1,1,0, AD]	[1,1,0, NAD]	[1,1,1, AD]	[1,1,1, NAD]	[1,1,1,I]
	[0,0,0, I]	0.326388889	0.298611111	0.118055556	0.111111111	0.046963277	0.064265537	0.03460452
5	[0,1,0, I]	0	0	0.314814815	0.296296296	0.125235405	0.171374765	0.09227872
	[1,1,0, I]	0	0	0	0	0.322033898	0.440677966	0.237288136
		[0,0,1, AD]	[0,0,1, NAD]	[0,1,1, AD]	[0,1,1, NAD]	[1,1,1, AD]	[1,1,1, NAD]	[1,1,1,I]
	[0,0,0, I]	0.263888889	0.326388889	0.125	0.138888889	0.040509259	0.067515432	0.037808642
6	[0,0,1, I]	0	0	0.305084746	0.338983051	0.098870056	0.164783427	0.092278719
	[0,1,1, I]	0	0	0	0	0.277777778	0.462962963	0.259259259

Figure 16: Absorption Probabilities for All Fixed Test Sequences

Sequence #		[0,0,0, I]	[1,0,0, I]	[1,1,0, I]
	[0,0,0, I]	1	0.239726027	0.095890411
1	[1,0,0, I]	0	1	0.4
	[1,1,0, I]	0	0	1
		[0,0,0, I]	[0,1,0, I]	[1,1,0, I]
	[0,0,0, I]	1	0.375	0.097222222
2	[0,1,0, I]	0	1	0.259259259
	[1,1,0, I]	0	0	1
		[0,0,0, I]	[1,0,0, I]	[1,0,1, I]
	[0,0,0, I]	1	0.243055556	0.097222222
3	[1,0,0, I]	0	1	0.4
	[1,0,1, I]	0	0	1
		[0,0,0, I]	[0,0,1, I]	[1,0,1, I]
	[0,0,0, I]	1	0.409722222	0.097222222
4	[0,0,1, I]	0	1	0.237288136
	[1,0,1, I]	0	0	1
		[0,0,0, I]	[0,1,0, I]	[1,1,0, I]
	[0,0,0, I]	1	0.375	0.145833333
5	[0,1,0, I]	0	1	0.388888889
	[1,1,0, I]	0	0	1
		[0,0,0, I]	[0,0,1, I]	[0,1,1, I]
	[0,0,0, I]	1	0.409722222	0.145833333
6	[0,0,1, I]	0	1	0.355932203
	[0,1,1, I]	0	0	1

Figure 17: Expected Time Periods in Transient States for All Fixed Test Sequences

4.2.2.a Experiment 2 Data Comparison

One-Way ANOVA tests were conducted to compare all six sequences' values of the absorption probabilities for states: [1, 1, 1, AD], [1, 1, 1, NAD], and [1, 1, 1, I]. These three states were compared to each other, because out of all the six tests these three states were the only absorption states that were similarly visited. The p-values for [1, 1, 1, AD], [1, 1, 1, NAD], and [1, 1, 1, I] were respectively 0.99, 0.89, and 0.97. The null hypothesis that states that all test means are equal, is not rejected and reveals that each different test sequence does not result in different absorption probabilities. This provides evidence that a fixed sequence does not impact the probability of patients contracting AD and not contracting AD. Table 20 shows the probabilities of contracting AD and not contracting AD (NAD) for each test sequence.

1st Sequence		**4th Sequence**	
Outcome	Probability	Outcome	Probability
AD	34%	AD	32%
NAD	31%	NAD	33%
2nd Sequence		**5th Sequence**	
Outcome	Probability	Outcome	Probability
AD	31%	AD	32%
NAD	35%	NAD	35%
3rd Sequence		**6th Sequence**	
Outcome	Probability	Outcome	Probability
AD	32%	AD	28%
NAD	35%	NAD	38%

Table 20: Totaled Fixed Test Sequence Classification Probabilities

These probabilities are compared to the 50% of patients contracting AD and the 50% of patients not contracting AD (NAD) from the ADNI data. It can be seen from Table 20 that the maximum difference from AD conversion among the test sequences and the patient data is 22% and the minimum difference of AD conversion against the patient data

is 10%. The best sequence for classifying AD patients is the 1st sequence and the worst sequence for classifying AD patients is the 6th sequence. The maximum difference between patient classification from the test sequences and the patient data for NAD contraction is 19% and the minimum difference is 6%. The best sequence for classifying NAD patients is the 6th sequence and the worst sequence for NAD classification is the 1st sequence. Similarly, to the comparison done in 4.2.1.a, the Inconclusive patient classification could not be conducted because the patient data did not contain that information.

From the comparison analysis seen above, the patient contraction of AD and non-contraction of AD (NAD) in the fixed test sequences are not as close to the original patient data classification as the original set thresholds from Figure 10 and the adjusted AD thresholds from Figure 14. The most accurate model of patient classification was conducted by the adjusted AD threshold model.

A different comparison was conducted pertaining to the expected time spent in transient states. The expected time spent in different test sequences could not be compared across all test sequences at once because each test sequence resulted in different transient states. Testing sequences were then paired based upon similar transient states. Figure 18 represents the plausible pairings.

Sequence #		[0,0,0, I]	[1,1,0, I]	Sequence #		[0,0,0, I]	[1,1,0, I]
1	[0,0,0, I]	1	0.09589	**2**	[0,0,0, I]	1	0.097222
	[1,1,0, I]	0	1		[1,1,0, I]	0	1

Sequence #		[0,0,0, I]	[1,0,1, I]	Sequence #		[0,0,0, I]	[1,0,1, I]
3	[0,0,0, I]	1	0.097222	**4**	[0,0,0, I]	1	0.097222
	[1,0,1, I]	0	1		[1,0,1, I]	0	1

Sequence #		[0,0,0, I]	[1,1,0, I]	Sequence #		[0,0,0, I]	[1,1,0, I]
5	[0,0,0, I]	1	0.145833	**2**	[0,0,0, I]	1	0.097222
	[1,1,0, I]	0	1		[1,1,0, I]	0	1

Sequence #		[0,0,0, I]	[0,0,1, I]	Sequence #		[0,0,0, I]	[0,0,1, I]
6	[0,0,0, I]	1	0.409722	**4**	[0,0,0, I]	1	0.409722
	[0,0,1, I]	0	1		[0,0,1, I]	0	1

Figure 18: Paired Expected Time Period Sequences

Sequences 1 and 2, and sequences 5 and 2 are the only sequences that have differing expected time periods. The significance of these differences was calculated by conducting two separate F-tests on both pair of sequences. Sequences 1 and 2 are not statistically significant because its F statistic, 1.003 is smaller than the F critical value, 161.45. This is interpreted that both expected time periods for [1, 1, 0, I] are the same. Sequences 5 and 6 are statistically different because its F value, 0.895, is larger than the F critical value, 0.0062. This demonstrates that the expected time periods for [1, 1, 0, I] from sequences 5 and 2 are different, as the expected time period is larger for sequence 5 than sequence 2. The comparison of expected time spent in transient periods could not be compared to the original thresholds and the adjusted AD thresholds because the number of transient states

was different among all three data sets. Additionally, the comparison against the patient data was not conducted because that information was not available.

CHAPTER 5: CONCLUSIONS AND FUTURE WORK

The importance of optimizing policy decisions about biomarker test administration impacts how soon a prognosis can be made regarding if a patient has contracted AD or not. AD has proven to be a disease that progresses over time. Along with time progression of a disease, there exists uncertain contributing factors to the contraction of AD. The need for medical decision-making models, such as Markov Chain models, allows the ability to model these stochastic factors. As referenced in 2.3, regarding the progression of HIV/AIDs, case studies have been used to demonstrate how Markov Chain models can be used in the healthcare industry. Markov Chain models allow researchers the ability to model the progression of diseases, optimize the procedure for prognosis, and decrease the associated healthcare costs. The STC had limitations that included the lack of ability to model dynamic factors associated with the progression of AD among different patient populations as well as the restriction of only modeling fixed test sequences. Based upon the biomarker tests' values from STCs, the Markov Chain model provides a more robust way to predict the progression of AD.

The methodology of the Markov Chain formulation was explained from the data collection to the calculation of the necessary probabilities needed to understand how many patients would contract the disease. Analysis was conducted based upon the probabilities to verify the accuracy of the Markov Chain model against a simulated model. The

experiment, using the Markov Chain model proved able to be simulated, based on different input parameters.

Based upon this verification, experiments were able to be conducted to demonstrate that alternating parameters of the Markov Chain model will yield different results in absorption probabilities and expected time periods spent in transient states. Absorption probabilities related information about how many patients would contract AD, not contract AD, and those that were inconclusive about contracting AD. The expected time periods spent in transient states demonstrated how long patients were expected to be unknowledgeable (Inconclusive) about their health state regarding AD. The first adjustment to the Markov Chain model was tightening the AD thresholds values and the second adjustment to the Markov Chain model was fixing certain test sequences. Revising the AD thresholds and implementing fixed test sequences to the Markov Chain model yielded different results and different interpretations. The adjustment of tightening the AD threshold, offered evidence that stricter AD thresholds resulted in fewer inconclusive states. On the other hand, fixed test sequences provided fewer transition states and demonstrated that fixed test sequences do not impact the absorption probabilities which affects the analysis of determining how many patients contract AD and those that do not. These experiments were additionally compared to the patient data set and revealed that the tightened AD threshold experiment proved to be the best model that closely matched the patient data classification.

There exist different opportunities for future work regarding this research. It would be beneficial to validate the conversion of AD results of fixed test sequences from the

Markov Chain model against the STC model's results. This verification was not conducted in this research because different data was provided to formulate the Markov Chain model versus the data tested by the STC model. Additionally, further optimization of the thresholds could be conducted with different fixed sequences. The decision-making process of which tests to administer would be conducted by converting the formulated Markov Chain model to a Markov Decision Process.

REFERENCES

[1] Selkoe, D. J. (2012). Preventing Alzheimer's Disease. *Science,337*(6101), 1488-1492. doi:10.1126/science.1228541

[2] Ballard, C., Gauthier, S., Corbett, A., Brayne, C., Aarsland, D., & Jones, E. (2011). Alzheimer's disease. *The Lancet,377*(9770), 1019-1031. doi:10.1016/s0140-6736(10)61349-9

[3] Si, Bing, et al. "A Sequential Tree-Based Classifier for Personalized Biomarker Testing of Alzheimer's Disease Risk." IISE Transactions on Healthcare Systems Engineering, doi:10.1080/24725579.2017.1367979.

[4] Gillis, D. (2007). New Criteria for Predicting Progression from Mild Cognitive Impairment to Alzheimer Disease. *Neurology Today,7*(11), 34-35. doi:10.1097/01.nt.0000280866.39572.54

[5] Basics of Alzheimer's Disease Prevention. (2010). *Journal of Alzheimer's Disease,20*(3), 687-688. doi:10.3233/jad-2010-091580

[6] Tan, Pang-Ning, et al. "Introduction to Data Mining." *Introduction to Data Mining*, Pearson, 2015, pp.145-146.

[7] Assumptions in a Normal Linear Model, www.ist.massey.ac.nz/dstirlin/CAST/CAST/HregnProblem/regnProblem1.html.

[8] H. Yang *et al*., "Healthcare Intelligence: Turning Data into Knowledge," in *IEEE Intelligent Systems*, vol. 29, no. 3, pp. 54-68, May-June 2014. doi: 10.1109/MIS.2014.45

[9] Lee, S., Ko, J., Tan, X., Patel, I., Balkrishnan, R., & Chang, J. (2014). Markov Chain Modelling Analysis of HIV/AIDS Progression: A Race-based Forecast in the United States. *Indian Journal of Pharmaceutical Sciences*, *76*(2), 107–115.

[10] Winston, Wayne L. "Markov Chains." *Operations Research: Applications and Algorithms*, Brooks/Cole, Thomson Learning, pp. 923–926.

[11] Banks, J. (2010). *Discrete-Event System Simulation*. Upper Saddle River: Prentice Hall.

[12] Chattin, Linda. (2015). Chapter 2: Data Summary and Presentation Sections 2.1 and 2.3 only [PowerPoint Slides]. Retrieved from https://myasucourses.asu.edu/webapps/blackboard/content/listContent.jsp?course_id=_310587_1&content_id=_11445964_1&mode=reset.

[13] Solberg, J. J. (2009). *Modeling Random Processes for Engineers and Managers*. Hoboken: John Wiley & Sons.

[14] Winston, W. L., & Goldberg, J. B. (2004). *Operations Research: Applications and Algorithms*. Belmont, CA: Thomson/Brooks/Cole.

[15] Pedrielli, Giulia. (2017). Models for Stochastic Systems [PowerPoint Slides]. Retrieved from https://myasucourses.asu.edu/webapps/blackboard/execute/content/file?cmd=view&content_id=_15349714_1&course_id=_347976_1.

[16] Chattin, Linda. (2015). Decision Making for Two Samples Chapter 5 [PowerPoint Slides]. Retrieved from https://myasucourses.asu.edu/webapps/blackboard/content/listContent.jsp?course_id=_310587_1&content_id=_11445964_1&mode=reset

[17] Vidakovic, B. (n.d.). Retrieved from https://www2.isye.gatech.edu/

[18] Tan, P., Steinbach, M., Karpatne, A., & Kumar, V. (2004). Introduction to Data Mining [PowerPoint Slides]. Retrieved from https://myasucourses.asu.edu/webapps/blackboard/content/listContent.jsp?course_id=_365695_1&content_id=_16629763_1